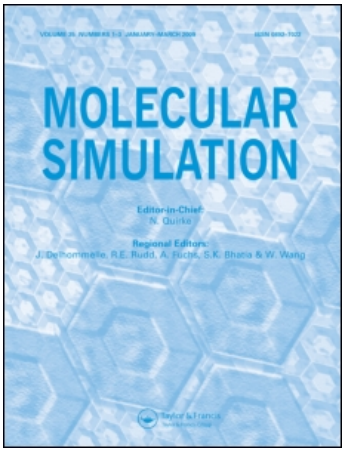

Molecular Simulation
Publication details, including instructions for authors and subscription information:
http://www.informaworld.com/smpp/title~content=t713644482

Modelling gas mixture adsorption in active carbons

M. B. Sweatman[a]; N. Quirke[b]
[a] Department of Chemical and Process Engineering, University of Strathclyde, Glasgow, UK [b] Department of Chemistry, Imperial College, London, UK

To cite this Article Sweatman, M. B. and Quirke, N.(2005) 'Modelling gas mixture adsorption in active carbons', Molecular Simulation, 31: 9, 667 — 681
To link to this Article: DOI: 10.1080/08927020500108296
URL: http://dx.doi.org/10.1080/08927020500108296

Molecular Simulation, Vol. 31, No. 9, August 2005, 667–681

Taylor & Francis
Taylor & Francis Group

Modelling gas mixture adsorption in active carbons

M. B. SWEATMAN* and N. QUIRKE†

*Department of Chemical and Process Engineering, University of Strathclyde, Glasgow G1 1XJ, UK
†Department of Chemistry, Imperial College, South Kensington, London SW7 2AY, UK

(Received December 2004; in final form January 2005)

We review recent progress made concerning the modelling of equilibrium gas mixture adsorption in activated carbons. Much of the discussion focuses on modern statistical mechanical methods, such as classical density functional theory and Monte-Carlo simulation, as well as the surface models employed, i.e. the surface characterisation, and we confine our attention to work that has been compared quantitatively with experiment. We will see that for less demanding scenarios, i.e. relatively simple gas mixtures adsorbed at supercritical temperatures, current methods are satisfactory. But further developments in our models and theories are probably needed to describe the adsorption of more complex adsorbates such as those involving water at room temperature.

Keywords: Active carbon; adsorption; isotherm prediction; gas mixture; density functional theory; Monte carlo simulation; surface model

1. Introduction

In this review we consider recent progress in the modelling of gas mixture adsorption in active carbons. Traditionally, adsorption onto surfaces is described by "isotherm" equations [1–9] that attempt to encode all the relevant phenomena with a few fitted parameters, largely ignoring the complex physics of non-uniform fluids interacting with non-uniform surfaces. These approaches have provided limited insight and, as a consequence, limited confidence. The advent of modern methods based on statistical mechanics and fast computers has radically changed this state of affairs. To a significant degree, the physics of adsorption is now well understood and today methods for modelling adsorption in active carbons are generally limited only by the complexity of the surface model, the patience of the modeller and the quality of experimental reference data. However, the addition of $n-1$ dimensions to the pure adsorption problem, where n is the number of components in the mixture, can make calculations much more difficult and time consuming than for the pure isotherm case. Yet an application might require predictions to be made quickly, in which case calculation of mixture adsorption isotherms using sophisticated approaches directly, involving Monte-Carlo (MC) simulation [10–12] for example, is out of the question particularly if there are several components in the mixture. So methods for predicting adsorption that are both fast and accurate are of great interest.

The most industrially important adsorbents generate high selectivity, i.e. they have a clear preference for adsorption of one gas component relative to another. Selectivity is influenced strongly by gas–surface interactions. So we will primarily be interested in the narrowest pores, called micropores, whose size is less than about 2 nm. The pores in active carbons cover a wide range of sizes, but it is generally micropores that dominate and give rise to useful adsorptive behaviour. Fluid behaviour in larger pores is interesting from a fundamental perspective. For example, hysterisis associated with capillary condensation can lead to unusual coexistence and percolation behaviour in systems not dominated by strong gas–surface interactions. But this behaviour and these materials are not the focus of this review.

When designing new materials the accuracy of gas adsorption prediction is required to be quantitative, not merely qualitative. So we concentrate here on methods that have been applied to make quantitative predictions for gas mixture adsorption in real materials. We will see that even the most modern methods are not completely satisfactory. For example, adsorption isotherms for some simple pure gases in activated carbons can be predicted

*Corresponding author. E-mail: martin.sweatman@strath.ac.uk

Molecular Simulation
ISSN 0892-7022 print/ISSN 1029-0435 online © 2005 Taylor & Francis Group Ltd
http://www.tandf.co.uk/journals
DOI: 10.1080/08927020500108296

with accuracy close to that of experiments at super- or near-critical temperatures. But the same confidence does not yet extend to significantly subcritical gases. Although popular and fast, a thermodynamic theory for predicting mixture adsorption, namely "ideal adsorbed solution theory" or IAST, is limited in its applicability. Fortunately, for active carbons an alternative, more versatile, accurate and robust approach based on classical density functional theory (DFT) has been devised. Consequently, the barrier to materials design optimisation is shifting towards their manufacture, i.e. our ability to produce large amounts of material that have nanoscopic properties within a specified tolerance.

The remainder of this review is structured as follows. In the following subsections we discuss some basic issues regarding the modelling of adsorption experiments. Then we turn briefly to DFT and MC methods for calculating adsorption for both pure and mixed gases on a given surface. We then deal with surface models that can be used in conjunction with DFT and MC to generate adsorption isotherms. Finally, we discuss in more detail methods for predicting gas mixture adsorption on the basis of pure component data, focussing on those methods that have been compared with experiment. We conclude with a summary.

2. Preliminaries

2.1. Surface characterization

Surface characterization is an important part of the modelling process. Little insight into the behaviour of adsorbates can be gained without it. The most common [1,2,13–15] experimental method for characterizing active carbons involves measurement of one or more adsorption isotherms of a "probe" adsorbent. The ideal probe will be attracted strongly to the surface to reduce experimental error, it will remain fluid at all locations in the adsorbent to avoid pore blocking and it will be sub-critical so that capillary condensation can be used to discriminate pore width. Generally, the probe will become more sensitive to pore width as its temperature is lowered towards its triple-point. But venturing too close to the triple-point runs the risk of pore-blocking [16] caused by freezing or slow dynamics. Traditionally [1,4,7], nitrogen at 77 K is used as a probe following the conventional BET method.

For polar molecules the polarity of the surface plays an important role in adsorption. The complex interaction between pore width and surface charge distribution might require several probes to be used to distinguish competing effects. For example, non-polar argon might be used to generate a PSD, while water adsorption could be used to assess surface polarity for the given PSD. Recent studies involving titration [17,18] are thought to provide greater detail with respect to particular surface functional groups (for example, nitrogen, phosphorus or oxygen functional groups). Other measurements that provide characteristics of the surface include X-ray diffraction and high-resolution transmission electron microscopy (HRTEM) from which average pair-distribution functions can be obtained, spectroscopy which also measures the type and number of functional groups present, temperature programmed desorption, electrokinetic measurements and immersion calorimetry. These experimental methods are not the focus of this review, but details concerning their application and further references can be found in [19] and [20].

Clearly, it is not possible to generate a model that describes every atom in a macroscopic sample of active carbon. The aim then is to create a model that captures the most significant features of the surface so that sufficiently accurate predictions can be made. Many modern studies employ a "pore-size distribution" (PSD) to characterise the pore network in a material. However, definitive statements about the pore network geometry should always be considered with caution for several reasons. Most importantly, it is not a well-defined property because the geometry of a curved surface is not independent of the adsorbate. Secondly, it is not yet possible to directly measure the pore network geometry with respect to any real nanoporous adsorbate. Instead, we can only make rather crude inferences on the basis of indirect measurements, such as adsorption isotherms and adsorption energies. And these measurements are often easily confused by competing influences such as pore width and the strength of adsorbate–surface interactions [21–23]. And finally, interpretation of these measurements is entirely dependent on our imposed models and their calibration.

2.2. Absolute and excess isotherms

Excess adsorption, N^{ex}, is the number of moles of adsorbate in an accessible volume in excess of the number of moles of adsorbate that would fill this volume if it had a uniform density equal to the bulk adsorbate density $\rho_{\mathrm{f}}^{\mathrm{b}}$, i.e.

$$N^{\mathrm{ex}} = N_{V_{\mathrm{f}}}^{\mathrm{tot}} - \rho_{\mathrm{f}}^{\mathrm{b}} V_{\mathrm{f}} \tag{1}$$

where $N_{V_{\mathrm{f}}}^{\mathrm{tot}}$ is the experimentally measured total number of moles of adsorbate in a volume V_{f} that includes all the accessible pore space and none of the inaccessible pore space. $N_{V_{\mathrm{f}}}^{\mathrm{tot}}$ is measured directly in an experiment, either gravimetrically or volumetrically, but V_{f} is not well-defined because it is impossible in an experiment to distinguish gas adsorbed in accessible pore space, $V_{\mathrm{f}}^{\mathrm{p}}$, from gas in the experimental bulk volume, $V_{\mathrm{f}}^{\mathrm{b}}$. So we can write

$$V_{\mathrm{f}} = V_{\mathrm{f}}^{\mathrm{p}} + V_{\mathrm{f}}^{\mathrm{b}} \tag{2}$$

As explained carefully by Neimark and Ravikovitch [24], it is standard practice to define V_{f} by measuring the total adsorption of helium at a particular pressure and temperature. If it is assumed that the excess adsorption of helium is zero then we have $V_{\mathrm{f}} = N_{V_{\mathrm{He}}}^{\mathrm{tot}} / \rho_{\mathrm{He}}^{\mathrm{b}}$ and using

equation (1) again

$$N^{\mathrm{ex}} = N^{\mathrm{tot}}_{V_{\mathrm{f}}} - \frac{\rho^{\mathrm{b}}_{\mathrm{f}}}{\rho^{\mathrm{b}}_{\mathrm{He}}} N^{\mathrm{tot}}_{V_{\mathrm{He}}} \tag{3}$$

All the quantities on the right hand side of equation (3) can be measured directly in an experiment. A problem with this definition is that it is well known that helium can experience significant adsorption, especially in the narrowest pores and at low temperature. So this definition of V_{f} and N^{ex} should be viewed as a calibration. This should be contrasted with the usual definition of excess adsorption in theoretical models

$$N^{\mathrm{ex}}_{\mathrm{the}} = N^{\mathrm{tot}}_{V_{\mathrm{the}}} - \rho^{\mathrm{b}}_{\mathrm{f,the}} V_{\mathrm{the}} \tag{4}$$

where V_{the} is the pore volume accessible to fluid in the theoretical model and $\rho^{\mathrm{b}}_{\mathrm{f,the}}$ is used to distinguish the modelled bulk density from the experimental bulk density at a particular pressure. So theoretical model predictions are exact when

$$N^{\mathrm{tot}}_{V^{\mathrm{p}}_{\mathrm{f}}} - N^{\mathrm{tot}}_{V_{\mathrm{the}}} = \rho^{\mathrm{b}}_{\mathrm{f}} \frac{N^{\mathrm{tot}}_{V^{\mathrm{p}}_{\mathrm{He}}}}{\rho^{\mathrm{b}}_{\mathrm{He}}} - \rho^{\mathrm{b}}_{\mathrm{f,the}} V_{\mathrm{the}} \tag{5}$$

For a perfect model $N^{\mathrm{tot}}_{V^{\mathrm{p}}_{\mathrm{f}}} = N^{\mathrm{tot}}_{V_{\mathrm{the}}}$ and $\rho^{\mathrm{b}}_{\mathrm{f}} = \rho^{\mathrm{b}}_{\mathrm{f,the}}$ in which case we must set $V_{\mathrm{the}} = N^{\mathrm{tot}}_{V^{\mathrm{p}}_{\mathrm{He}}}/\rho^{\mathrm{b}}_{\mathrm{He}}$ to ensure that perfect agreement with experiment is obtained. For a perfect model $N^{\mathrm{tot}}_{V^{\mathrm{p}}_{\mathrm{He}}}$ can be obtained from the model itself. Neimark and Ravikovitch [24] argue that this definition should be used for any model. They show that the adsorption of helium in the low-pressure (Henry's law) limit depends strongly on temperature, so the temperature at which $N^{\mathrm{tot}}_{V^{\mathrm{p}}_{\mathrm{He}}}$ is obtained experimentally can have a dramatic impact on calculated values of N^{ex} for supercritical or near-supercritical adsorbates. Essentially the same conclusions are reached by Myers and Monson [25]. They also suggest that helium calibration should be standardised. As pointed out by Ozdemir *et al.* [26] the above arguments are correct only for a rigid adsorbent. For adsorbents that swell, such as some types of clay and gel, V_{the} should be reduced by a volume equal to the amount of swelling. However, active carbons are usually thought to be quite rigid and are generally modelled as such.

2.3. Confined fluid phase behaviour

Fluids in pores exhibit richer phase behaviour compared to the bulk phase. The counterparts of equilibrium bulk phase transitions like the gas–liquid transition are generally shifted to other bulk pressures and temperatures when fluid is confined to a pore. The magnitude of this shift depends on the pore size, geometry and the nature of the fluid–surface interaction. A modified [27] form of Kelvin's equation predicts this shift for the liquid–gas transition for a cylindrical pore

$$k_{\mathrm{B}}T \ln(P_{\mathrm{sat}}/P) = \frac{2\gamma_{\mathrm{lg}} \cos\theta}{R(\rho_{\mathrm{l}} - \rho_{\mathrm{g}})} \tag{6}$$

provided R, the pore radius, is very large compared to the adsorbate particle size. Here, θ is the "contact angle" [28] required to stabilise a droplet of liquid on an isolated surface, γ_{lg} is the gas–liquid surface tension at bulk coexistence, ρ_{l} and ρ_{g} are the bulk liquid and gas densities at coexistence and P_{sat}/P is the ratio of the bulk saturation pressure to the confined saturation pressure.

For fluids confined in pores with relatively strong fluid–surface interactions, like nitrogen in the graphitic pores of active carbons, the pressure at which capillary condensation occurs steadily reduces with pore size. For pore sizes that we are concerned with the Kelvin equation is no longer accurate [29,30] and alternative theories are needed. An accurate theory should be able to reproduce the correct condensation pressure for a pore of any size and be able to predict the modulation of this transition caused by packing effects in the smallest pores. In addition, surface phase transitions that have no bulk counterpart such as pre-wetting are possible for sufficiently smooth surfaces. These transitions are sensitive to the nature of both fluid–fluid and fluid–surface interactions and they can influence the shifted bulk transitions [31]. For active carbons capillary condensation is the most useful transition because it is very sensitive to pore size.

Phase behaviour in amorphous nanoscopic materials is complicated further by pore–pore interactions [32–36]. For example, the equilibrium capillary condensation pressure of a pore can be reduced due to adsorption in neighbouring, smaller pores. This proximity effect can be important for systems in which fluid–fluid interactions are relatively strong compared to fluid–surface interactions (xenon adsorbed in a high porosity xerogel [32] for example). In active carbons the high density of carbon atoms forming the graphitic surfaces leads to relatively strong fluid–surface interactions, so this proximity effect is less significant for the adsorption of simple gases, such as nitrogen and carbon dioxide, and many studies choose to ignore it. However, for more complex adsorbates, particularly those with longer ranged electrostatic interactions (e.g. water), these pore–pore interactions might be significant.

2.4. Poor equilibration

Poor equilibration is a factor that complicates both experimental and theoretical studies of adsorption. It covers several phenomena, including metastability, pore blocking and poor diffusion. It is further complicated by the connectivity of the network of pores. Each of these mechanisms can lead to hysteresis where the adsorption and desorption curves are not identical.

The relative importance of metastability versus pore-blocking as the prime hysterisis mechanism in amorphous adsorbents has been debated for decades. Early pore network analysis methods [37] often relied on pore-blocking,

but recent work by Kierlik and colleagues [32,34], Monson and colleagues [35,36] and Neimark and co-workers [38–40] demonstrates that metastability is sufficient to account for various types of hysteresis seen in experiment, i.e. that pore-blocking might not be significant. Moreover, Sarkisov and Monson [41] question the traditional picture of pore-blocking for simple fluids in "ink-bottle" geometries on the basis of molecular dynamics results.

Fortunately, hysteresis due to metastability is less important or absent for many active carbons and simple gas mixtures. Using a mean-field DFT Ravikovitch and colleagues [42] find that metastability generated hysteresis of nitrogen at 77 K in spherical silica pores is essentially a mesoscopic phenomenon that generally occurs in pores larger than about 6 nm. Similar conclusions are likely for other materials, including active carbons, and subcritical gases, although the precise onset of hysteresis with pore width will be sensitive to the particular system. So for simple gases and microporous active carbons, including carbon molecular sieves, metastability hysterisis can be neglected. But for active carbons with significant mesoporosity such as carbon aerogels, or for more complex adsorbates such as water, hysterisis might well be important for significantly sub-critical gases.

For complex systems poor diffusion can be significant even in micropores. For example, studies [43] involving water adsorption in activated carbons that have polar surface sites have shown that water adsorbed at these sites can potentially block the entrances of pores (although the effect on diffusion through these blocked pore entrances was not addressed in this work). Nakashima *et al.* [44] report activated diffusion in a particular activated carbon using carbon dioxide as a probe at 273 K. Moreover, if fluid becomes very dense within a pore it can freeze [45] at temperatures shifted relative to the bulk freezing temperature, thereby blocking access to connected pores. This is exacerbated by relatively strong fluid–surface interactions [46–48] and by pore-junctions [49] and pits [50], i.e. the kind of heterogeneous surfaces expected in active carbons. Indeed, there is speculation [16,51] that the most commonly used probe gas, nitrogen at 77 K, either freezes, becomes glassy or highly viscous when adsorbed in the narrowest pores of active carbons at sub-atmospheric pressure. This could have a major impact on traditional pore characterization experiments [1,2,6] that routinely use nitrogen at 77 K, including the BET analysis of surface area. The work of Radhakrishnan *et al.* [46,47,52] indicates [16] that to avoid pore-blocking of this kind probes should be employed at a temperature well above their bulk triple-point temperature. Clearly, a compromise temperature is required so that the adsorbate is sufficiently mobile while remaining sufficiently sensitive to the surface and pore width; a reasonable choice might be a third of the way between the triple and critical points.

2.5. Molecular sieving

No two adsorbates experience the same amorphous surface. Molecular sieving can result if one adsorbate can reach regions of the pore network that are inaccessible to another adsorbate because its molecules are too large to fit through any of the connecting pores. This effect is clearly very dependent on the connectivity of the pore network. In addition, kinetic molecular sieving [53] can occur if the diffusion of one component through the carbon pore network is much greater than another. We do not consider these factors.

3. Adsorption isotherms

We focus in this section on modern methods that can generate adsorption isotherms for any given external potential, i.e. inert surface. We do not discuss the many popular engineering or empirical isotherms [1–9].

3.1. DFT

Classical DFT [54] is the most successful theory of non-uniform equilibrium fluids. Since its initial development for quantum systems and extension to classical systems [55], it has been one of the most useful tools for understanding confined fluid behaviour alongside molecular simulation. The central ideas and main developments are described in several books [28,54,56,57] and are repeated only briefly here.

The density functional formalism [55] is developed in the grand-canonical ensemble, which is the natural ensemble for discussing inert adsorbents. The grand potential, Ω, is expressed as a functional of the set of one-body densities, $\{\rho(\mathbf{r})\}$, where $\mathbf{r}$ represents all static degrees of freedom (positions, orientations etc.) of a molecule, as follows

$$\Omega[\{\rho(\boldsymbol{r})\}] = F[\{\rho(\mathbf{r})\}] + \sum_i \int \mathrm{d}\mathbf{r}\rho_i(\mathbf{r})\left(V_i^{\mathrm{ext}}(\mathbf{r}) - \mu_i\right) \quad (7)$$

where F is the intrinsic Helmholtz free-energy functional, V_i^{ext} is an external one-body potential, μ_i is the chemical potential and i labels the component of the mixture.

The global minimum of Ω with respect to variation of $\{\rho(\mathbf{r})\}$ at fixed chemical potential, temperature and external potential corresponds to the equilibrium Ω_0 and equilibrium set $\{\rho^0(\mathbf{r})\}$. So specification of $\Omega[\{\rho(\mathbf{r})\}]$ (or equivalently $F[\{\rho(\mathbf{r})\}]$) and a method for finding its global minima are central to many DFT studies. The ideal gas contribution, F^{id}, is known for rigid particles

$$\begin{aligned} F &= F^{\mathrm{id}} + F^{\mathrm{ex}} \\ &= k_{\mathrm{B}}T\sum_i \int \mathrm{d}\boldsymbol{r}\rho_i(\mathbf{r})\left(\ln\left(\Lambda_i^3\rho_i(\mathbf{r})\right) - 1\right) + F_{\mathrm{HS}}^{\mathrm{ex}} + F_{\mathrm{p}} \end{aligned} \quad (8)$$

where Λ_i is the thermal de Broglie wavelength, leaving only the excess contribution, F^{ex}, to be specified.

For spherical models of the gas molecules of interest to us the short-range repulsive "core" contribution to F^{ex} is usually treated by a hard-sphere term, F^{ex}_{HS}, with the remainder treated by a perturbation, F_p.

The development of approximate hard-sphere functionals warrants a separate review, so we provide only brief details here. Less attention has been paid to treatment of the perturbation contribution [58,59]. Indeed, in every application of DFT to materials characterization known to us the same perturbation term is used

$$F_p = \frac{1}{2}\sum_{ij}\int\int d\mathbf{r}_1\, d\mathbf{r}_2 \rho_i(\mathbf{r}_1)\rho_j(\mathbf{r}_2)\phi^p_{ij}(r_{12}) \qquad (9)$$

where $\phi^p_{ij}(r)$ is the perturbation potential and $r_{12} = |r_1 - r_2|$. If a Lennard–Jones potential is used, then according to the WCA [56] convention

$$\phi^p_{ij}(r) = \begin{cases} 4\varepsilon_{ij}(x^{-12} - x^{-6}); & x > 2^{1/6} \\ -\varepsilon_{ij}; & x \le 2^{1/6} \end{cases} \qquad (10)$$

where $x = r/\sigma_{ij}$, and σ and ε are the Lennard–Jones length and energy parameters, respectively. Usually, a cutoff in the range of $\phi^p_{ij}(r)$ is employed to avoid lengthy numerical integrations. This type of mean-field perturbation is very common throughout the DFT literature because of its simplicity, but it is not that accurate [58], particularly at low temperatures [59].

The development of DFT methods in materials characterization has closely followed the development of hard-sphere functionals. The first such study [60] employed a pure fluid local density approximation for this contribution

$$F^{ex}_{HS} = \int d\mathbf{r} f^{ex}_{HS}(\rho(\mathbf{r}); d) \qquad (11)$$

where f^{ex}_{HS} is the excess free-energy density of a uniform hard-sphere fluid with hard-sphere diameter d. But this functional cannot describe the packing of particles in very narrow pores and so is not a good choice for accurate studies of nanoporous materials. Consequently, despite its simplicity, it is rarely used [61,62].

Much greater accuracy can be achieved, at greater numerical expense, with a weighted density approximation (WDA) or "non-local" DFT. The "smoothed density approximation" (SDA2) of Tarazona [63] is one such approach and is known [40,64,65] to be quite accurate for adsorption studies. Most DFT characterization studies have used this functional [13,29,66–71]. It ascribes the excess free-energy per particle, ψ^{ex}, at a point in the fluid non-local character

$$F^{ex}_{HS} = \int d\mathbf{r}\rho(\mathbf{r})\psi^{ex}_{HS}(\bar{\rho}(\mathbf{r}); d) \qquad (12)$$

where

$$\bar{\rho}(\mathbf{r}_1) = \int dr_2 \rho(\mathbf{r}_2) w(r_{12}; \bar{\rho}(\mathbf{r}_1)) \qquad (13)$$

and

$$w(r;\rho) = w_0(r) + \rho w_1(r) + \rho^2 w_2(r). \qquad (14)$$

The density independent weight functions, w_0, w_1 and w_2, are chosen to accurately reproduce thermodynamic and structural properties of the uniform fluid, including the Carnahan-Starling equation of state [56], and have a range equal to d.

Recently, the fundamental measure functional (FMF), developed originally by Rosenfeld [72,73] and by Kierlik and Rosinberg [74], has been employed [64] in characterization studies. It has several advantages over the SDA2 functional including its accuracy and efficiency. Although it has become the functional of choice for fundamental studies of simple fluid behaviour, it has yet to be used to predict adsorption in real materials, so we refer the interested reader to other articles [16,54,64,75].

Combining equations (7) and (8) with the minimal Ω principle gives the Euler-Lagrange (EL) equation for the densities

$$\rho^0_i(\mathbf{r}) = \rho_{bi}\exp\left(-\beta\left(V^{ext}_i(\mathbf{r}) - \mu^{ex}_i + \left(\frac{\delta F^{ex}}{\delta\rho_i(\mathbf{r})}\right)_{\{\rho^0(\mathbf{r})\}}\right)\right) \qquad (15)$$

where the excess chemical potential $\mu^{ex}_i = \mu_i - k_B T \ln(\Lambda_i^3\rho_{bi})$ and ρ_{bi} is the bulk density corresponding to μ_i. Because the last term on the right-hand-side depends on $\{\rho^0(\mathbf{r})\}$, which is also the solution on the left-hand-side, the EL equations can be solved by simple (Picard) iteration. Alternatively, if a gradient (Newton) method [76] is used then many fewer iterations might be required to reach a desired level of accuracy, but at greater numerical expense for each iteration.

In the above theories the Lennard–Jones parameters, σ and ε, and the hard-sphere diameter, d, can be chosen independently. Several theoretical methods have been suggested for fixing d, given σ and ε, such as the Barker-Henderson [56] (BH), Weeks-Chandler-Anderson [57] (WCA), Lado [77] and Rosenfeld [78] prescriptions. However, given the inherent inaccuracies in the above approximations, particularly the mean-field perturbation term equation (9), it is more appropriate to fit the free parameters to reference data, i.e. experiment or molecular simulation data. Ravikovitch *et al.* [64] compared several methods and concluded that fitting $\sigma = d$ and ε to experimental data for bulk liquid–gas coexisting pressures and densities for a range of temperatures was the most convenient and accurate approach.

For mixtures of Lennard–Jones fluids cross-interaction parameters are usually calculated via the Lorentz-Berthelot (LB) combining rules

$$\sigma_{ij} = (\sigma_i + \sigma_j)/2; \quad \varepsilon_{ij} = \sqrt{\varepsilon_i\varepsilon_j} \qquad (16)$$

This can be successful for gas–gas interactions dominated by dispersion forces, for example those between methane and nitrogen. But for less symmetric

molecular interactions, such as between methane and water, it is likely that cross-interactions will need to be fitted to reference mixture data.

3.2. MC simulation

The equilibrium statistical mechanics of a Hamiltonian can be solved, to within statistical error, with MC and molecular dynamics simulations [10–12]. Not surprisingly, these methods, and MC simulation in particular, are popular for characterization and adsorption studies. Due to the popularity of books [10–12] in this field and detailed articles [79,80] we will not dwell on the basics here.

Whereas with DFT the grand-canonical ensemble is the most convenient choice, with MC simulation in particular the choice of ensemble is completely open. The grand-canonical ensemble is best suited to rigid, inert adsorbents whereas the osmotic ensemble [81] may be suited to swelling materials.

A molecular MC simulation is an attempt to sample the relevant microstates of an ensemble in accordance with the laws of equilibrium statistical mechanics [82] i.e. the Boltzmann equation. Usually, many millions of states are sampled by starting the system from a particular configuration (described by the system volume and specification of each degree of freedom for each initial molecule) and performing a sequence of small moves (a Markov chain). In a grand-canonical ensemble Monte-Carlo (GCMC) simulation three types of move are attempted at random. Attempts are made to randomly displace, create or destroy particles resulting in equilibration of temperature and chemical potential. Usually, moves are required to satisfy microscopic reversibility, so creation and destruction attempts are attempted with equal probability.

With today's computing power simulations of several hundred to several thousand particles are typical. Molecules are often modelled with multi-site combinations of Lennard–Jones potentials and partial charges. To enable such a relatively small system to mimic a macroscopic system requires the use of periodic boundary conditions. Provided the system is sufficiently large these periodic boundaries will not significantly affect results. For "long-range" interactions, such as those between coulombic charges, special techniques (such as the Ewald method) [11] are needed to make progress. Several of these techniques have been tested recently by Seaton and co-workers [83] in the context of water adsorption in slit-pores using GCMC simulation. They find that a method due to Heyes and van Swol [84] is the most efficient in their application, and see no reason why this should not be a general result.

As the density of the system increases it becomes increasingly unlikely that attempted creation or destruction moves will be accepted because the probability of formation of a cavity at equilibrium reduces with increasing density. Nitrogen adsorbed in narrow graphitic pores at 77 K and 1 bar, for example, is so dense that it may well be close to freezing. Not only might this manifest as an experimental difficulty associated with poor diffusion, but it also hinders simulations because the low probability of creation and destruction results in poor statistics even for very long simulations. Many approaches have been suggested in the literature to combat this difficulty, including cavity bias [85] excluded volume mapping [86] and staged insertion [87].

To reproduce experiment accurately any molecular model must be calibrated. In gas adsorption experiments we need adsorbate molecular models to be accurate both for gas-like and liquid-like densities. Often, molecular models are calibrated by requiring that bulk gas–liquid coexistence properties like density and pressure are accurately reproduced. Essentially, this means finding bulk gas and liquid states for a particular molecular model that have identical chemical potential and pressure. Before the invention of the Gibbs ensemble [88] this would typically have involved calculating the chemical potential and pressure along each phase branch separately [10], a lengthy process particularly if the molecular model is to be optimised to reproduce experiment. However, the Gibbs ensemble [10,88–95] has revolutionised this process as it generates coexisting phases without need of an interface in a single simulation.

The Gibbs ensemble answers the question "What is the most likely, or equilibrium, partitioning of particles between two (separated) simulation boxes if their total number, the total volume and temperature are held constant?" Essentially, it explores the minimum of the total Helmholtz free-energy, or equivalently the minimum of the sum of the Helmholtz free-energies of each simulation box. The Gibbs ensemble has also been used to study phase equilibria in confined systems [96–99], and modified versions, called "gauge-cell" simulations [100,101] are able to explore hysteresis loops in detail.

The liquid–gas phase diagram of a molecular model can be sketched quite efficiently by performing Gibbs ensemble MC (GEMC) simulations for a sufficient number of temperatures, or by implementing a thermodynamic scaling method [102]. Alternatively, the thermodynamic integration route of Mehta and Kofke [103] can be employed to generate the coexistence curve given an initial point on the curve generated by GEMC.

4. Adsorbent models

In this section we discuss surface models that have been used in conjunction with DFT and MC simulation to make adsorption predictions for real materials. All of these models take the surface to be inert and are applied in the grand-canonical ensemble. They effectively define an appropriate external potential.

4.1. Polydisperse independent ideal pore models

By far the most popular modern model for characterizing porous adsorbents is the polydisperse ideal pore model.

Quite simply, the adsorption in a number of independent ideal pores with a range of sizes, H, is added together (or integrated over for a continuous distribution) to give the total amount adsorbed per gram of material at a particular pressure P,

$$N(P) = \int_0^\infty \mathrm{d}H f(H) v(H,P) \tag{17}$$

Here, $f(H)$ is called a PSD, $v(H,P)$ is the "kernel" of "local" *excess* isotherms (for comparison with experiment) and the mass of material is measured in a vacuum. The kernel is pre-generated and the PSD is optimised to minimise the difference, usually measured in terms of the root-mean-square (rms) deviation, between the experimental isotherm and the isotherm calculated from equation (17).

The simplest geometries that generate a confined pore space are slits, cylinders and spheres. In a slit pore the external potential, $V_i^{\mathrm{ext}}(z)$, is the sum of contributions from each wall,

$$V_i^{\mathrm{ext}}(z) = V_i^w(z) + V_i^w(H - z) \tag{18}$$

where z measures distance normal to the plane of the slit. To preserve transverse symmetry the gas–solid potential is usually constructed by "smearing" out individual gas–solid atom contributions. The well-known Steele potential [104] performs this integration for each layer of a graphitic surface to arrive at the rather accurate gas–solid interaction

$$V_{\mathrm{i}}^{\mathrm{w}}(z) = 2\pi\rho_{\mathrm{w}}\sigma_{\mathrm{iw}}^2\varepsilon_{\mathrm{iw}}\Delta_{\mathrm{w}} \times \left(\frac{2}{5}\left(\frac{\sigma_{\mathrm{iw}}}{z}\right)^{10} - \left(\frac{\sigma_{\mathrm{iw}}}{z}\right)^{4} - \frac{\sigma_{\mathrm{iw}}^4}{3\Delta_{\mathrm{w}}(0.61\Delta_{\mathrm{w}}+z)^3}\right) \tag{19}$$

where ρ_{w} is the density of atoms in the wall, Δ_{w} is the inter-layer spacing between graphitic sheets (usually taken to be $114\,\mathrm{nm}^{-3}$ and 0.335 nm, respectively [5,104]) and σ_{iw} and $\varepsilon_{\mathrm{iw}}$ are the gas–solid interaction length and strength parameters, respectively. These parameters can be determined by fitting to experiment, just as with the gas–gas parameters. But we leave discussion of this until later.

If the experimental pore volume is calibrated with helium an effective "chemical" pore width for helium will be required, as discussed earlier. The excess adsorption is then calculated as

$$N(P) = \int_0^H \mathrm{d}H f(H)\left(v^{\mathrm{ab}}(H,P) - \frac{\rho_{\mathrm{b}}(P)}{\rho_{\mathrm{He}}} v_{\mathrm{He}}^{\mathrm{ab}}(H)\right) \tag{20}$$

where $v^{\mathrm{ab}}(H,P)$ is the *absolute* local adsorption and $v_{\mathrm{He}}^{\mathrm{ab}}(H)$ is the local adsorption for helium at the calibration temperature and pressure. However, many studies of this type avoid using a helium calibrated pore width and instead use an arbitrary chemical pore width, for example $H - 0.34\,\mathrm{nm}$, which leads to inconsistencies with experiment.

Active carbons are usually modelled with the polydisperse ideal slit-pore model. While the precise nature of the pore surface must depend on the precursor and treatment, there is recent evidence from high-resolution electron microscopy [105,106] (HREM) that for non-graphitising carbons the pore surface is formed from curved fullerene-like fragments with 5, 6 and 7-membered rings. A random arrangement of these elements produces a rather tortuous pore-space. Whatever the nature of the surface the polydisperse slit-pore model can be quite successful [15] for activated carbons and some simple near-supercritical gases.

The first DFT method [60] employed a local DFT equation (11) to model the repulsive contribution to the Helmholtz free energy. But more recent DFT work [14,29,42,64,66,107,108] has used one of the "non-local" theories described earlier, i.e. either the SDA2 or FMF for hard-spheres (augmented by a simple mean-field term for attractive forces equation (9)). Despite the undoubted gains made with using DFT to generate the kernel, there is no *explicit* evidence that the DFTs and models described earlier in this chapter are able to accurately predict adsorption, either of the same gas used to generate the PSD at other temperatures or of other gases at any temperature. While DFT has proved popular for fundamental studies of fluid behaviour in pores and for characterization studies there are no studies, to our knowledge, that make predictions for either pure or mixed gas adsorption in real materials using DFT. We can expect, given the accuracy of non-local DFTs in ideal pores for simple fluids, that it might be quite accurate for predicting adsorption of simple fluids in active carbons. But we cannot expect similar accuracy for more complex fluids with significantly non-spherical molecular shapes or with electrostatic moments, such as butane and water. Further work is needed to establish whether current DFT methods are sufficient to model a range of gases in active carbons, or whether more sophisticated functionals and models are required.

Several studies [15,51,71,109–111] use the polydisperse ideal-pore model and GCMC simulation to generate the kernel. Despite some encouraging results, it seems that all this work suffers the same limitation, i.e. that gas–surface interactions are calibrated to reproduce adsorption on low-surface area carbons and applied to analyse adsorption on high-surface area carbons that might have quite different *effective* gas–surface interaction strengths.

This point is discussed in recent work by us [112]. We show that if the same characterization method is used to characterise active carbons and Vulcan, a low surface area carbon, then predictions are poor on Vulcan when gas–surface interactions are calibrated to an active carbon, and vice-versa. Here, we provide some pure gas adsorption prediction results in addition to those in Ref. [112] using precisely the same methods. Figure 1 shows the predicted isotherms for two active carbons. Satisfactory agreement is obtained, particularly in figure 1a. We have tested nearly 20 different active carbons and generally we find that adsorption predictions can be made with accuracy rivalling

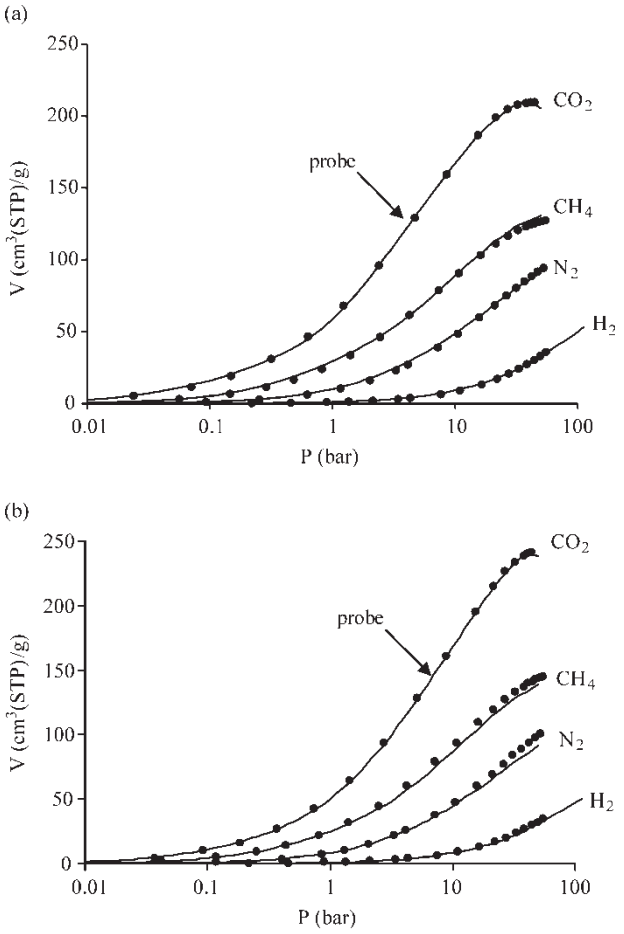

Figure 1. Adsorption isotherms of carbon dioxide, methane, nitrogen and hydrogen on two representative high surface area carbons. The methane, nitrogen and hydrogen isotherms (lines) are predictions based on carbon dioxide slit-PSDs and MC simulation kernels. Gas–surface interaction strength parameters are calibrated to a reference active carbon (see Ref. [112]). Symbols are experiment—carbon dioxide measurements up to about 45 bar (the saturation pressure of carbon dioxide at this temperature is about 57 bar) while the other measurements are up to about 55 bar.

that in figure 1a and better than in figure 1b. Figure 2 shows predictions for Vulcan using the same approach. These results indicate that the *effective* strength of gas–surface interactions in high surface area carbons are quite different

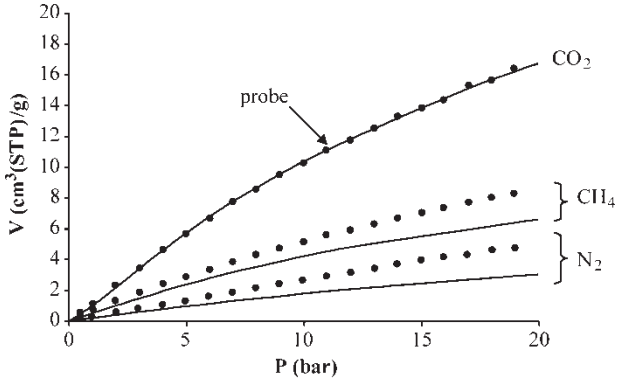

Figure 2. As for figure 1 except that the adsorbent is Vulcan (and no hydrogen data is available for this material). Also, pressure is on a linear scale and is measured up to 19 bar only.

to those in low-surface area carbons (see Ref. [112] for a fuller discussion), although it is clearly desirable that the corresponding experiments on which this finding is based be repeated to corroborate this. The origin of this *apparent* change in effective gas–surface interaction strengths between low and high surface area carbons is not clear although we can speculate about several possibilities. It might be that the effective pair potential (calibrated to a low surface area carbon) between a fluid atom and a wall atom is modified by the close proximity of a second wall in active carbons—an effective three-body effect, or that the surfaces of low and high surface area carbons are quite different regarding their bonding structure and chemistry, or even that the degree of wall curvature, pits, intersections etc. can influence these effective interactions.

Although promising, adsorption prediction for these gases at much lower, sub-critical temperatures is a much needed, more stringent test of the model and methods. Also, the above gases are relatively simple in that their electrostatic interactions are relatively weak. The simple slit-PSD model could well need modification if it is to describe adsorption of more polar gases such as water.

4.2. 3D models

Despite the undoubted success of the polydisperse independent pore model for mimicking the behaviour of some systems, for example the adsorption of weakly polar near- or super-critical gases on activated carbon [15,109,112] it is known to be inadequate for a range of other important systems. Its failure is the result of two factors; (a) the modelled uniformity of individual pores, and (b) the independence of these pores.

In real materials there will be both geometric and energetic non-uniformities that result in phenomena that the ideal pore model cannot capture. Indeed, it cannot even clearly distinguish energetic from geometric non-uniformity or one kind of geometry from another [21–23]. Maddox and co-workers [49] have investigated the influence of pore-junctions on adsorption of a model of nitrogen at 77 K using molecular simulation. They found that this geometric non-uniformity resulted in pore-blocking and that similarly sized independent pores did not exhibit this phenomenon. Papadopoulous *et al.* [113], Kozak *et al.* [114], and Gelb [115] have studied the influence of boundary conditions on adsorption in smooth-walled pores of finite length using MC simulation and mean-field DFT. Essentially, they find that ideal pores of infinite length exhibit enhanced hysteresis because the formation of menisci is suppressed. For strongly dipolar molecules, like water, Brennan and colleagues [43,116] find that energetic non-uniformities can potentially lead to pore blocking. And Kierlik and colleagues [32–34] have demonstrated that pore–pore interactions can potentially significantly effect hysterisis.

Clearly, characterization of nanoporous materials in terms of a polydisperse independent pore model is a gross approximation. For activated carbons high-resolution

electron micrographs [105,106] indicate that the slit-pore model might be a reasonable starting point. But there can be great value in developing surface models that address specific issues such as energetic or geometric non-uniformity or pore-pore interactions. However, a surface model that can capture all of these effects is likely to very complex. If energetic and geometric non-uniformity are predominantly short-range in nature and if pore–pore interactions are long-range then an accurate model will probably be described over a wide range of length scales. Essentially, an accurate model will need to capture nanostructure and network topology. Recent articles [16,19,116] have addressed the development of detailed 3-D surface models in some depth. Although these models have provided insight into problems of a qualitative nature potential pore blocking of active carbons by water for example [117], results published to date from these models are not as accurate as results obtained with the simple polydisperse slit pore model for predicting pure adsorption isotherms, and none of these models have been used to predict mixture adsorption in active carbons, so we will not describe them here. Nevertheless, it is certainly possible that future work with these advanced models might reverse this situation.

5. Predicting gas mixture adsorption

Active carbons are used for a variety of purposes on an industrial scale, but most of them involve the separation of one fluid component from another. The problem that fluid mixtures present concerns the additional degrees of freedom generated by each component after the first. For pure fluids we need specify only the bulk pressure and temperature, so an adsorbed phase diagram is relatively easy to map. But for mixtures it becomes increasingly difficult to map the adsorbed phase diagram as the number of fluid components increases.

If we consider one method for predicting pure fluid adsorption, the adsorption integral equation (17), and adapt it to mixtures we find that we need to specify an $n+1$-dimensional kernel (at a fixed temperature) for an n-component mixture. If we represent the kernel at a fixed temperature by a matrix of, say, 10 elements for pressure and each bulk mole fraction we find that the number of data entries is 10^{n+1}, a rather large number, even for small n. So it is quite impractical to try to pre-generate the kernel by calculating each data entry using a numerically intensive method such as MC simulation or even non-local DFT. Alternatively, the mixture kernels for a specific bulk composition could be generated as required, but this would still require many hours or days of computer time whenever a new mixture calculation is performed.

On the other hand, it is unlikely that any method for predicting mixture adsorption in nanoporous amorphous materials will be successful generally unless it models the behaviour of fluid mixtures at the nanoscale. So our goal is to create a method that is both accurate at the nanoscale and very quick. This is precisely why this problem is difficult, interesting and important. An accurate and fast method would be of use both in probing the physical chemistry of mixed adsorption and in practical applications to, for example, adsorbent design.

Every approach to this problem in the literature is based on modelling the adsorption of the pure components and using a fast theory to make predictions for the mixture. The modelling of pure component adsorption was discussed briefly in the previous sections. Many have attempted to extend "empirical" pure adsorption equations to mixtures. For example, the Langmuir [9,118–121], Dubinin-Radushkevich [122], Dubinin-Astakhov [123] and Toth [124] isotherms and neural-network [125] and virial [9,126–128] methods have been adapted in this way to analyse a variety of gas mixture systems. In these approaches parameters describing the adsorbed gas mixture are determined by fitting to the pure component data. We do not detail these largely empirical methods here.

One of the most significant theories for predicting gas mixture adsorption is based on a thermodynamic treatment of adsorption at a surface. In 1965 Myers and Prausnitz [129] invented Ideal Adsorbed Solution Theory (IAST), which is essentially an extension of ideal solution theory [130] to adsorption. The IAST equations can be written succinctly as

$$P^0_{\mathrm{bi}}(\Omega_{\mathrm{a}})x_{\mathrm{ai}} = P_{\mathrm{b}}x_{\mathrm{bi}} \;\; ; \;\; \frac{1}{N_{\mathrm{a}}} = \sum_i \frac{x_{\mathrm{ai}}}{N^0_{\mathrm{ai}}} \qquad (21)$$

where $P^0_{\mathrm{bi}}(\Omega_{\mathrm{a}})$ is the pressure required to generate the adsorbed phase grand potential Ω for pure component i, P_{b} is the bulk pressure of the mixture, x_{ai} and x_{bi} are the compositions of the adsorbed and bulk phases respectively, and N_{a} and N^0_{ai} are the total amount of mixture and of pure component i respectively in the adsorbed phase.

This theory for the adsorbed mixture takes as its only input the pure component isotherms $P^0_{\mathrm{bi}}(\Omega_{\mathrm{a}})$, all at the same temperature. Unfortunately, predictions for gas mixture adsorption at this temperature are limited by the input data to regions in the pressure–bulk composition space. There is no constraint on how the input isotherms are described. For example, one could fit straight-line segments between a set of data-points. But usually the input data is described in terms of a smooth adsorption equation such as the Langmuir [118,131,132], Dubinin-Radushkevich [133] or Toth [131] isotherms. In 1995, Cracknell and Nicholson [134] suggested that the original theory should be re-cast in terms of the total, or absolute, grand potential rather than the "spreading pressure", which is the negative of the excess grand-potential per unit area. Vuong and Monson [135] arrived at the same conclusion, which was later proved by us [136]. However, in the original 1965 paper the formal thermodynamic framework is based on absolute quantities, hence our use of the grand potential in equation (21).

IAST makes no assumptions about the nature of the adsorbent other than it is inert. IAST itself is not based on any nanoscopic model, but the pure component isotherms can be. This means that IAST can be combined with a model of the surface, such as a polydisperse pore model. This attractive feature has been used by several groups [67,137–139] to describe gas mixture adsorption prediction beyond the standard application of IAST. There is some evidence that a surface model defined in terms of a PSD [139] seems to be preferred [138] to one defined in terms of a distribution of gas–surface interaction energies [140,141] (ED). However, we note that this heterogeneous IAST (or HIAST) approach can seriously reduce the pressure–bulk composition region within which solutions can be obtained.

Accurate prediction of mixture adsorption in active carbons requires a theory that models both the surface and gas at a molecular level. Or, in the language of AST (an exact generalisation of IAST), a theory is required that can calculate the effect of the surface on activity coefficients [142]. Given the success of non-local DFT and molecular simulation in modelling pure gas adsorption one should expect them to be successful in predicting mixed gas adsorption as well. Using a slit-PSD generated from the pure methane adsorption isotherm and a GCMC methane kernel Gusev and O'Brien [143] find that they are unable to satisfactorily predict the adsorption of methane/ethane gas mixtures at 308 K in BPL-6 activated carbon at moderate to high pressures using the same PSD and a GCMC mixture kernel, although they find better agreement with experiment at low pressure. Davies and Seaton [144] used the same methods to study these gases on a range of activated carbons. They find that pure component adsorption is predicted quite well for both gases for a range of temperatures above 293 K up to high pressure (about 30 bar or so) on several carbons using a PSD generated from the pure ethane isotherm at 293 K. This is despite using gas–surface interactions that have been optimised for adsorption on low-surface area carbons. They also find that selectivity is predicted quite well at relatively low pressure (1 bar or less), but is less satisfactory at higher pressures. They compare the use of MC simulation with IAST for predicting mixture adsorption and find close agreement, presumably because the mixture is relatively ideal under the conditions analysed. Heuchel and co-workers [145] analyse carbon dioxide/methane mixtures at ambient temperature up to 17 bar. They find that, generally, better predictions for gas mixture adsorption can be obtained as more and more input data is used, i.e. using several pure gas isotherms as input is better that using just one. They attribute this to obtaining a more accurate PSD as more input data is used.

Despite some encouraging results, these are not particularly stringent tests of the model because the probe gas (ethane or carbon-dioxide at ambient temperature) is only marginally sub-critical and is used to predict adsorption of the probe gas at higher temperatures and methane adsorption at super-critical temperatures to moderate pressure only (less than 20 bar). Mixture adsorption prediction is also limited to low or moderate pressures. Overall, we find that predictions for mixed gas adsorption in this work are somewhat disappointing considering the level of sophistication. In all of this MC simulation work a likely cause of error is due to calibration of the molecular models. In each case gas–surface interaction parameters are fitted to reproduce adsorption on a low-surface area carbon. The assumption is that this parameterisation is valid for high-surface area carbons. Results in Ref. [112] indicate that this assumption is highly optimistic. In any event, these MC methods are numerically intensive and much quicker methods are desirable.

There have been no attempts to predict gas mixture adsorption in nanoporous materials with a non-local DFT of the type detailed earlier. But recently we have found some success with a particularly simple, "trimmed-down", non-local DFT [136] that is able to predict the adsorption of pure gases in active carbons at a range of temperatures [112] and gas mixtures in active carbons [146] both accurately and quickly using a PSD as input. In summary, this success stems from two key advances. The first concerns calibration of the molecular models, that is we calibrate gas–surface interactions to reproduce pure gas adsorption on a reference high-surface area carbon (as discussed in the previous section on pure gas adsorption). The second concerns our novel and simple slab-DFT.

The slab-DFT, as with all DFT approaches applied to materials characterization, treats gas molecules as hard-spheres with a mean-field perturbation. Although accurate non-local theories for hard-sphere fluids exist, they are numerically intensive and inappropriate for quick calculations. We approximate the intrinsic excess Helmholtz free-energy with equations (9)–(11)

$$F^{\mathrm{ex}} = \int \mathrm{d}\mathbf{r} f_{\mathrm{HS}}^{\mathrm{PYex}}(\{\rho(\mathbf{r}\}) + \frac{1}{2}\sum_{\mathrm{ij}} \int\int \mathrm{d}\mathbf{r}_1\, \mathrm{d}\mathbf{r}_2 \rho_{\mathrm{i}}(\mathbf{r}_1)\rho_{\mathrm{j}}(\mathbf{r}_2)\phi_{\mathrm{ij}}^{\mathrm{p}}(r_{12}) \qquad (22)$$

where $f_{\mathrm{HS}}^{\mathrm{PYex}}$ is the Percus-Yevick [56] excess compressibility equation of state for bulk hard-sphere mixtures. To simplify matters further we adopted the slit-pore geometry and symmetrically parameterised the density into three slabs. In this respect our slab-DFT has parallels with the MSAM model of Gusev and co-workers [131], which divides pore space into two regions, a strongly adsorbed region and the remainder.

Our model is presented schematically in figure 3. The density slabs are described by the set (H_{p}, δH, ρ_{1i}, ρ_{2i}, ρ_{3i}, σ_{bi}, $\delta\sigma_{\mathrm{bi}}$, z_3), where each element is non-negative. Parameters with a subscript "i" can be different for each fluid component, otherwise they are the same for all components. The slit width, H_{p}, describes the physical width of the slit, i.e. H_{p} is the distance normal to the walls

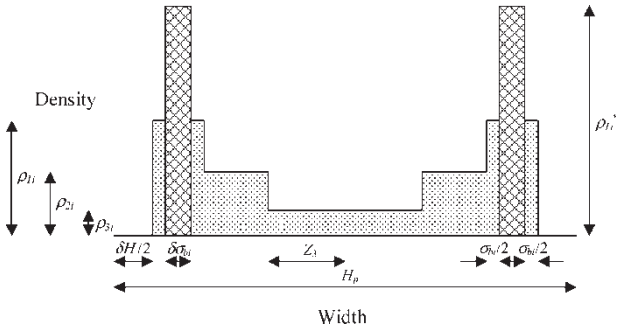

Figure 3. Schematic diagram of the slab-DFT model used to predict gas adsorption given a PSD as input in Refs. [136], [112] and [146]. This model is described in the text.

between wall atom centres. The region where the density is zero, described by $\delta H = H_p - H_c$, prohibits fluid particles from overlapping wall particles. The three regions or "slabs" of density represent (1) a monolayer of fluid strongly adsorbed at the wall with density ρ_{1i} and width $z_{1i} = \min(\sigma_{bi} + \delta\sigma_{bi}, H_c/2)$, (2) a thick layer of adsorbed fluid with density ρ_{2i}, and (3) the remaining fluid in the centre of the slit with density ρ_{3i} and width z_3.

For both the external potential and ideal gas contributions of slab 1 to the grand potential (see equations (7) and (8)) we transform slab1 so that it has width $\delta\sigma_{bi}$ while conserving the total number of particles, i.e. it has density $\rho^*_{1i} = \rho_{1i} z_{1i}/\delta\sigma_{bi}$. This is represented by the hashed region in figure 3. Because of this transformation of slab 1 for the external potential and ideal gas contributions only, in effect our prescription for F^{ex} is a crude non-local approximation. In summary, the grand potential is written [136]

$$\Omega = F^{ex} + 2A\sum_i \left\{ \begin{array}{l} \delta\sigma_{ib}\rho^*_{1i}\left(V_i^{ext} + \ln(\Lambda_i^3\rho^*_{1i}) - \mu_{ib} - 1\right) \\ +z_{2i}\rho_{2i}\left(\ln(\Lambda_i^3\rho_{2i}) - \mu_{ib} - 1\right) \\ +z_3\rho_{3i}\left(\ln(\Lambda_i^3\rho_{3i}) - \mu_{ib} - 1\right) \end{array} \right\} \quad (23)$$

where $z_{2i} = H_c/2 - z_{1i} - z_3$ and V_i^{ext} is the strength of gas–surface interactions. Minimisation of equation (23) with respect to the density with all other parameters held fixed, i.e. variation of (ρ_{1i}, ρ_{2i}, ρ_{3i}, z_3) at fixed (T, H_p, δH, σ_{bi}, $\delta\sigma_{bi}$, σ_{ai}, ε_{ai}, V_i^{ext}, ρ_b, x_{bi}), gives the equilibrium state according to this slab-model.

The bulk LJ parameter set, (σ_{bi}, ε_{bi}), is determined by fitting to pure bulk fluid reference pressure–density isotherms for a given temperature, T, with $H_p \to \infty$. The adsorbed parameter set is determined by estimating δH and $\delta\sigma_{bi}$ (see Refs. [136] and [146]), fixing V_i^x by fitting to the low-density limit of each pure fluid adsorption isotherm, and then fitting (σ_{ai}, ε_{ai}) to the entire range of each pure fluid adsorption isotherm. We set $d_i = \sigma_{ai}$, where σ_{ai} is the *effective* size of an adsorbed particle of type i and also define ε_{ai}, the *effective* interaction energy of an adsorbed particle of type i. So σ_{ai} and ε_{ai} are determined separately for each slit width, H_p. The Lorentz-Berthelot mixing rules equation (16) are used to model cross-interaction parameters for LJ interactions. We define the slab-DFT model in this way so that it can accurately and quickly reproduce the complex adsorption behaviour seen in adsorption kernels generated with MC simulation for a wide range of gases. Also note that we have used the LB rules to describe cross-interactions for convenience, and that greater accuracy might be achieved by calibrating these interactions to reproduce appropriate bulk mixture data.

We compared IAST against this slab-DFT and found that the slab- DFT [136] was significantly more accurate for predicting the adsorption of a model of a non-ideal gas mixture, carbon-dioxide and hydrogen (modelled with multiple LJ and partial charge sites), in ideal graphitic slit-pores. For relatively ideal gas mixtures, such as a model of methane and carbon dioxide, there was little difference in accuracy. Although the IAST approach was still quicker by far, our slab-DFT was sufficiently quick to be considered interactive, i.e. mixture isotherms in an ideal slit pore could be generated in under a second on a desktop PC. This result for highly non-ideal but relatively simple gas mixtures in ideal pores is encouraging, but the acid test is application to a real adsorbent. Accordingly, we performed several tests for a range of active carbons. First, we tested [112] the ability of the slab-DFT to convert a kernel generated with MC simulation at one temperature to a kernel at another temperature. We found that the slab-DFT was quite accurate for carbon-dioxide, nitrogen and methane, but less accurate for hydrogen at temperatures between 276 and 333 K, based on 293 K MC kernels. Figure 4 shows another example of this kind of test for a different active carbon. We expect [112] hat this behaviour can be improved by tuning the $\delta\sigma_{bi}$ parameter separately for each gas (by fitting to heat of adsorption data, for example), rather than

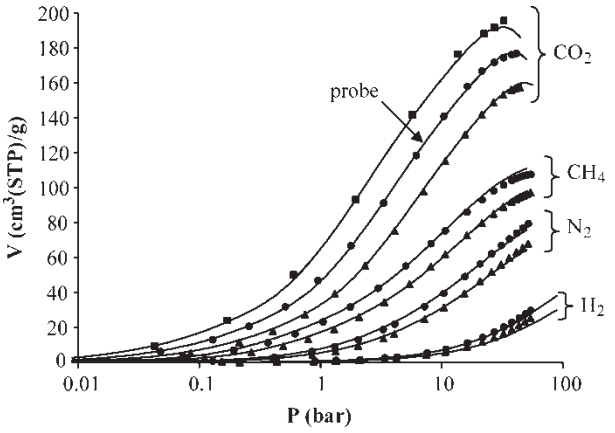

Figure 4. Adsorption isotherms on another active carbon at 276 K (squares), 293 K (circles) and 313 K (triangles). The predicted isotherms (lines) are based on a 293 K carbon dioxide slit-PSD and slab-DFT kernels for each gas at each temperature (see Ref. [112]). Gas–surface interaction strength parameters are calibrated to a reference active carbon (see Ref. [112]). Symbols are experiment −276 K measurements are up to 38 bar (the saturation pressure of carbon dioxide at this temperature), the others are as for figure 1.

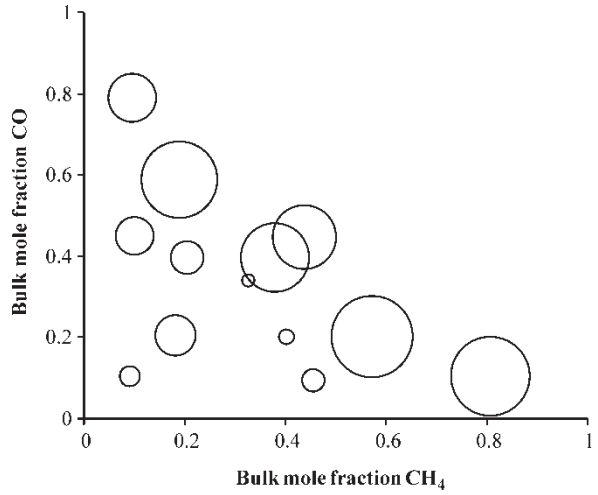

Figure 5. Predictions for the adsorption of ternary mixtures of CO_2, CH_4 and CO in an active carbon at 303 K and about 31 bar for a number of different bulk phase mole fractions. The area of each circle is proportional to the rms error in the adsorbed mole fractions of the mixture predicted with a slit-PSD and the slab-DFT. The slit-PSD is generated from a 303 K pure CO_2 isotherm while the kernels at 303 K are generated with the slab-DFT, which is parameterised to a 293 K MC simulation kernel. The largest circle corresponds to a rms error of 0.036.

adopting a "one-size fits all" approach [136]. Then, we tested [146] the slab-DFT's performance for some simple binary mixtures of CO_2, N_2 and CH_4 in two active carbons up to about 40 bar. The same gas and graphitic slit-pore models and methods outlined in the previous section concerning pure gas adsorption are used. We found that predictions made using a PSD based on just one carbon dioxide probe isotherm as input were satisfactory. Here, we provide some additional results for a ternary mixture of CO_2, CH_4 and CO at 303 K on an active carbon. Figure 5 shows the rms error in the predicted mole fractions of the adsorbed mixture for a number of mixtures with different bulk phase mole compositions. For these results the mixture kernels at 303 K are generated with the slab-DFT, which is parameterised at 293 K.

These results are encouraging, just like the pure gas results in the previous section. However, adsorption predictions for significantly sub-critical gas-mixtures would present a more severe test of the model. And it is not clear what modifications to the slab-DFT model and free energy functionals would be needed to allow modelling of more complex mixtures, such as water/alkane mixtures.

6. Conclusions

The adsorption of gas in active carbons is a complex process. A great deal of research in the past into this problem has tended to be based on extremely simplified modelling both in terms of the surface and adsorption isotherms. This is still the case today, although the more sophisticated approaches covered in this chapter seem to be gaining wider acceptance.

Active carbons are the most important industrial adsorbents and so it is no surprise that there is a great deal of research in this area. It seems somewhat fortunate that for these materials a relatively simple model of the surface, i.e. the polydisperse independent slit-pore model, is reasonably successful for modelling the adsorption of simple gases, at least at super- or near-critical temperatures. But this does not mean that this strategy will necessarily be successful for other materials or more complex adsorbates or lower temperatures. For example, materials that swell significantly might well require an altogether different approach. And even for inert surfaces the polydisperse independent pore model is inadequate for systems where it is important to distinguish energetic and geometric heterogeneity, or where pore-pore interactions are important (in hysteretic systems for example). In this case the more advanced and numerically intensive 3D models of active carbons are certainly useful, at least from a qualitative perspective, for understanding the more complex adsorption phenomena, and with further developments these models might yet become quantitatively accurate.

The simple "slab-DFT" model developed by us based on the polydisperse independent slit-pore model seems to fulfil many of the requirements outlined in the introduction, i.e. it is quite fast and accurate, at least for the simple gas mixtures analysed in this chapter. But its suitability for more complex systems, i.e. sub-critical or polar gas or long-alkane adsorption in active carbons is yet to be assessed. For these more complex adsorbates, and for the more detailed 3D models mentioned above, the venerable IAST approach of Myers and Prausnitz is, at first glance, well suited because it does not require definition of molecular models of either adsorbate or adsorbent. Unfortunately, there can be little confidence in this approach for the same reasons, and it is rather inflexible. So for these complex systems the more numerically demanding weighted DFT and MC simulation approaches described earlier that are often applied to fundamental studies of adsorption behaviour are recommended if speed is not important. The difficult problem of designing approaches that are both fast and accurate for complex systems has yet to be solved.

References

[1] F. Rouquerol, J. Rouquerol, K. Sing. *Adsorption by Powders and Porous Solids*, Academic Press, New York (1999).
[2] S.J. Gregg, K.S.W. Sing. *Adsorption, Surface Area and Porosity*, Academic Press, London (1991).
[3] D.M. Young, A.D. Crowell. *Physical Adsorption of Gases*, Butterworths, London (1962).
[4] A. Dabrowski. Adsorption—from theory to practice. *Adv. Colloid Interface Sci.*, **93**, 135 (2001).
[5] W.A. Steele. *The Interaction of Gases with Solid Surfaces*, Pergamon Press, Oxford (1974).
[6] D.M. Ruthven. *Principles of Adsorption and Adsorption Processes*, Wiley, Chichester (1984).
[7] H. Jankowska, A. Swiatkowski, J. Choma. *Active Carbon*, Ellis Horwood, New York (1991).
[8] R.C. Bansal, J. Donnet, F. Stoeckli. *Active Carbon*, Marcel Dekker, New York (1988).
[9] R.T. Yang. *Gas Separation by Adsorption Processes*, Imperial College Press, Singapore (1997).
[10] B. Smit, D. Frenkel. *Understanding Molecular Simulation: from Algorithms to Applications*, Academic Press, New York (1996).

[11] M.P. Allen, D.J. Tildesley. *Computer Simulation of Liquids*, Clarendon Press, Oxford (1987).

[12] D. Nicholson, N.G. Parsonage. *Computer Simulation and the Statistical Mechanics of Adsorption*, Academic Press, London (1982).

[13] M.L. Lastoskie, K.E. Gubbins. Characterization of porous materials using molecular theory and simulation. *Adv. Chem. Eng.*, **28**, 203 (2001).

[14] P.I. Ravikovitch, A. Vishnyakov, R. Russo, A.V. Neimark. Unified approach to characterization of microporous carbonaceous materials from N_2, Ar and CO_2 adsorption isotherms. *Langmuir*, **16**, 2311 (2000).

[15] M.B. Sweatman, N. Quirke. Characterization of porous materials at ambient temperatures and high pressure. *J. Phys. Chem. B*, **105**, 1403 (2000).

[16] M.B. Sweatman, N. Quirke. *Handbook of Theoretical and Computational Nanotechnology*, American Scientific Publishers, Stevenson Ranch, CA, In press.

[17] C. Contescu, J. Jagiello, J.A. Schwarz. Heterogeneity of proton binding-sites at the oxide solution interface. *Langmuir*, **9**, 1754 (1997).

[18] J. Jagiello, T.J. Bandosz, J.A. Schwartz. Carbon surface characterization in terms of its acidity constant distribution. *Carbon*, **32**, 1026 (1994).

[19] T.J. Bandosz, M. Biggs, K.E. Gubbins, K. Kaneko, K. Thomson. In *Chemistry and Physics of Carbon*, **29**, L.R. Radovic (Ed.), Marcel Dekker, New York (2003).

[20] R.T. Yang. *Adsorbents: Fundamentals and Applications*, Wiley-Interscience, Hoboken (2003).

[21] G.M. Davies, N.A. Seaton. The effect of the choice of pore model on the characterization of the internal structure of microporous carbons using pore size distributions. *Carbon*, **36**, 1473 (1998).

[22] W. Gac, A. Patrykiejew, S. Sokolowski. Monte-Carlo study of adsorption in energetically and geometrically non-uniform slit-like pores. *Thin Solid Films*, **298**, 22 (1997).

[23] M.J. Bojan, W.A. Steele. Computer simulation in pores with rectangular cross-sections. *Carbon*, **36**, 1417 (1998).

[24] A.V. Neimark, P.I. Ravikovitch. Calibration of pore volume in adsorption experiments and theoretical models. *Langmuir*, **13**, 5148 (1997).

[25] A.L. Myers, P.A. Monson. Adsorption in porous materials at high pressure: Theory and experiment. *Langmuir*, **18**, 10261 (2002).

[26] E. Ozdemir, B.I. Morsi, K. Schroeder. Importance of volume effects to adsorption isotherms of carbon dioxide on coals. *Langmuir*, **19**, 9764 (2003).

[27] R. Evans, U.M.B. Marconi. The role of wetting films in capillary condensation and rise: influence of long-range forces. *Chem. Phys. Lett.*, **114**, 415 (1985).

[28] J.S. Rowlinson, B. Widom. *Molecular Theory of Capillarity*, Oxford University Press, Oxford (1982).

[29] M.L. Lastoskie, K.E. Gubbins, N. Quirke. Pore-size distribution analysis of microporous carbons—a density functional theory approach. *J. Phys. Chem.-US*, **97**, 4786 (1993).

[30] J.P.R.B. Walton, N. Quirke. Capillary condensation: a molecular simulation study. *Mol. Sim.*, **2**, 361 (1989).

[31] R. Evans, U.M.B. Marconi. Capillary condensation versus pre-wetting. *Phys. Rev. A*, **32**, 3817 (1985).

[32] E. Kierlik, P.A. Monson, M.L. Rosinberg, G. Tarjus. Adsorption hysteresis and capillary condensation in disordered porous solids: a density functional study. *J. Phys.: Condens. Matter*, **14**, 9295 (2002).

[33] E. Kierlik, M.L. Rosinberg, G. Tarjus, P. Viot. Equilibrium and out-of-equilibrium (hysteretic) behavior of fluids in disordered porous materials: Theoretical predictions. *Phys. Chem. Chem. Phys.*, **3**, 1201 (2001).

[34] E. Kierlik, P.A. Monson, M.L. Rosinberg, L. Sarkisov, G. Tarjus. Capillary condensation in disordered porous materials: Hysteresis versus equilibrium behavior. *Phys. Rev. Lett.*, **87**, 055701 (2001).

[35] L. Sarkisov, P.A. Monson. Lattice model of adsorption in disordered porous materials: Mean-field density functional theory and Monte Carlo simulations. *Phys. Rev. E*, **65**, 011202 (2002).

[36] H.J. Woo, L. Sarkisov, P.A. Monson. Mean-field theory of fluid adsorption in a porous glass. *Langmuir*, **17**, 7472 (2001).

[37] N.A. Seaton. Determination of the connectivity of porous solids from nitrogen sorption measurements. *Chem. Eng. Sci.*, **46**, 1895 (1991).

[38] A.V. Neimark, P.I. Ravikovitch, A. Vishnyakov. Inside the hysterisis loop: Multiplicity of internal states of confined fluids. *Phys. Rev. E*, **65**, 031505 (2002).

[39] P.I. Ravikovitch, A.V. Neimark. Characterization of nanoporous materials from adsorption and desorption isotherms. *Colloid Surface A*, **187**, 11 (2001).

[40] A.V. Neimark, P.I. Ravikovitch, A. Vishnyakov. Adsorption hysteresis in nanopores. *Phys. Rev. E*, **62**, R1493 (2000).

[41] L. Sarkisov, P.A. Monson. Modeling of adsorption and desorption in pores of simple geometry using molecular dynamics. *Langmuir*, **17**, 7600 (2001).

[42] P.I. Ravikovitch, A.V. Neimark. Density functional theory of adsorption in spherical cavities and pore size characterization of templated nanoporous silicas with cubic and three-dimensional hexagonal structures. *Langmuir*, **18**, 1550 (2002).

[43] J.K. Brennan, K.T. Thomson, K.E. Gubbins. Adsorption of water in activated carbons: Effects of pore blocking and connectivity. *Langmuir*, **18**, 5438 (2002).

[44] M. Nakashima, S. Shimada, M. Inagaki, T.A. Centeno. On the adsorption of CO_2 by molecular-sieve carbons—volumetric and gravimetric studies. *Carbon*, **33**, 1301 (1995).

[45] H. Dominguez, M.P. Allen, R. Evans. Monte-Carlo studies of the freezing and condensation transitions of confined fluids. *Mol. Phys.*, **96**, 209 (1999).

[46] R. Radhakrishnan, K.E. Gubbins, M. Sliwinska-Bartkowiak. Global phase diagrams for freezing in porous media. *J. Chem. Phys.*, **116**, 1147 (2002).

[47] R. Radhakrishnan, K.E. Gubbins, M. Sliwinska-Bartkowiak. Effect of the wall-fluid interaction on freezing of confined fluids: Toward the development of a global phase diagram. *J. Chem. Phys.*, **112**, 11048 (2000).

[48] M. Schneemilch, N. Quirke, J.R. Henderson. Wetting of nanopatterned surfaces: The hexagonal disk surface. *J. Chem. Phys.*, **120**, 2901 (2004).

[49] M.W. Maddox, N. Quirke, K.E. Gubbins. A molecular simulation study of pore networking effects. *Mol. Sim.*, **19**, 267 (1997).

[50] A.R. Turner, N. Quirke. A grand canonical Monte Carlo study of adsorption on graphitic surfaces with defects. *Carbon*, **36**, 1439 (1998).

[51] M.B. Sweatman, N. Quirke. Characterization of porous materials by gas adsorption: Comparison of Nitrogen at 77 K and carbon dioxide at 298 K for activated carbon. *J. Phys. Chem. B*, **105**, 1403 (2001).

[52] R. Radhakrishnan, K.E. Gubbins. Free energy studies of freezing in slit pores: an order parameter approach using Monte Carlo simulation. *Mol. Phys.*, **96**, 1249 (1999).

[53] M.A. de la Casa-Lillo, B.C. Moore, D. Cazorla-Amoros, A. Linares-Solano. Molecular sieve properties obtained by cracking of methane on activated carbon fibers. *Carbon*, **40**, 2489 (2002).

[54] R. Evans. *Fundamentals of Inhomogeneous Fluids*, D. Henderson (Ed.), Marcel Dekker, New York (1992).

[55] R. Evans. The nature of the liquid-vapour interface and other topics in the statistical mechanics of classical non-uniform fluids. *Adv. Phys.*, **28**, 143 (1979).

[56] J.P. Hansen, I.R. McDonald. *Theories of Simple Liquids*, Academic, London (1986).

[57] M.B. Sweatman. Analysis of free energy functional density expansion theories. *Mol. Phys.*, **98**, 573 (2000).

[58] M.B. Sweatman. Weighted density functional theory for simple fluids: Supercritical adsorption of a Lennard–Jones fluid in an ideal slit pore. *Phys. Rev. E*, **63**, 031102 (2001).

[59] M.B. Sweatman. Weighted density functional theory for simple fluids: pre-wetting of a Lennard–Jones fluid. *Phys. Rev. E*, **65**, 011102 (2002).

[60] N.A. Seaton, J.P.R.B. Walton, N. Quirke. A new analysis method for the determination of the pore-size distribution of porous carbons from nitrogen adsorption measurements. *Carbon*, **27**, 853 (1989).

[61] D.L. Valadares, F.R. Reinoso, G. Zgrablich. Characterization of active carbons: The influence of the method in the determination of the pore size distribution. *Carbon*, **36**, 1491 (1998).

[62] P.N. Aukett, N. Quirke, S. Riddiford, S.R. Tennison. Methane adsorption on microporous carbons—a comparison between experiment, theory and simulation. *Carbon*, **30**, 913 (1992).

[63] P. Tarazona. Free-energy density functional for hard-spheres. *Phys. Rev. A*, **31**, 2672 (1985).

[64] P.I. Ravikovitch, A. Vishnyakov, A.V. Neimark. Density functional theories and molecular simulations of adsorption and phase transitions in nanopores. *Phys. Rev. E*, **64**, 011602 (2001).

[65] A.V. Neimark, P.I. Ravikovitch, A. Vishnyakov. Bridging scales from molecular simulations to classical thermodynamics: density functional theory of capillary condensation in nanopores. *J. Phys.: Condens. Matter*, **15**, 347 (2003).

[66] S. Scaife, P. Kluson, N. Quirke. Characterization of porous materials by gas adsorption: Do different molecular probes give different pore structures? *J. Phys. Chem. B*, **104**, 313 (2000).

[67] P. Kluson, S. Scaife, N. Quirke. The design of microporous graphitic adsorbents for selective separation of gases. *Sep. Purif. Technol.*, **20**, 15 (2000).

[68] M.L. Lastoskie, N. Quirke, K.E. Gubbins. Structure of porous adsorbents: Analysis using density functional theory and molecular simulation. *Stud. Surf. Sci. Catal.*, **104**, 745 (1997).

[69] P. Kluson, S. Scaife. Evaluation of adsorption properties of low surface area carbons—comparison of experiments with a theoretical study. *J. Porous Mat.*, **9**, 115 (2002).

[70] R.J. Dombrowski, D.R. Hyduke, M.L. Lastoskie. Pore size analysis of activated carbons from argon and nitrogen porosimetry using density functional theory. *Langmuir*, **16**, 5041 (2000).

[71] N. Quirke, S.R.R. Tennison. The interpretation of pore-size distributions of microporous carbons. *Carbon*, **34**, 1281 (1996).

[72] Y. Rosenfeld. Free-energy model for the inhomogeneous hard-sphere fluid mixture and density-functional theory of freezing. *Phys. Rev. Lett.*, **63**, 980 (1989).

[73] S. Phan, E. Kierlik, M.L. Rosinberg, B. Bildstein, G. Kahl. Equivalence of 2 free-energy models for the inhomogeneous hard-sphere fluid. *Phys. Rev. E*, **48**, 618 (1993).

[74] E. Kierlik, M.L. Rosinberg. Free-energy density functional for the inhomogeneous gard-sphere fluid—application to interfacial adsorption. *Phys. Rev. A*, **42**, 3382 (1990).

[75] M. Schmidt. Geometry-based density functional theory—an overview. *J. Phys.: Condens. Matter*, **15**, S101 (2003).

[76] L.J.D. Frink, A.G. Salinger. Two- and three-dimensional nonlocal density functional theory for inhomogeneous fluids I. Algorithms and parallelization. *J. Comput. Phys.*, **159**, 407 (2000).

[77] F. Lado. A local thermodynamic criterion for the reference-hypernetted chain equation. *Phys. Lett. A*, **89**, 196 (1982).

[78] Y. Rosenfeld. Free energy model for inhomogeneous fluid mixtures: Yukawa-charged hard-spheres, general interactions, and plasmas. *J. Chem. Phys.*, **98**, 8126 (1993).

[79] D. Nicholson. Using computer simulation to study the properties of molecules in micropores. *J. Chem. Soc. Farad. Trans.*, **92**, 1 (1996).

[80] M.B. Sweatman, N. Quirke. Modelling gas adsorption in slit-pores using Monte Carlo simulation. *Mol. Sim.*, **27**, 295 (2001).

[81] F.A. Escobedo. Simulation and extrapolation of coexistence properties with single-phase and two phase ensembles. *J. Chem. Phys.*, **113**, 8444 (2000).

[82] R.P. Feynman. *Statistical Mechanics*, Perseus Books, Reading, MA (1998).

[83] M. Jorge, N.A. Seaton. Long-range interactions in Monte-Carlo simulation of confined water. *Mol. Phys.*, **100**, 2017 (2002).

[84] D.M. Heyes, F. van Swol. The electrostatic potential and field in the surface region of lamina and semi-infinite point-charge lattices. *J. Chem. Phys.*, **75**, 5051 (1981).

[85] D.H.L. Yau, S.Y. Liem, K.Y. Chan. A contact cavity-biased method for grand-canonical Monte-Carlo simulations. *J. Chem. Phys.*, **101**, 7918 (1994).

[86] G.L. Deitrick, L.E. Scriven, H.T. Davis. Efficient molecular simulation of chemical potentials. *J. Chem. Phys.*, **90**, 2370 (1989).

[87] D.A. Kofke, P.T. Cummings. Quantitative comparison and optimization of methods for evaluating the chemical potential by molecular simulation. *Mol. Phys.*, **92**, 973 (1997).

[88] A.Z. Panagiotopoulos. Direct determination of phase coexistence properties by Monte-Carlo simulation in a new ensemble. *Mol. Phys.*, **61**, 813 (1987).

[89] A.Z. Panagiotopoulos. Direct determination of fluid-phase equilibria by simulation in the Gibbs ensemble—a review. *Mol. Sim.*, **9**, 1 (1992).

[90] F.A. Escobedo. Simulation of bulk, confined, and polydisperse systems. I. A unified methodological framework. *J. Chem. Phys.*, **115**, 5642 (2001).

[91] T. Kristof, J. Liszi. Alternative Gibbs ensemble Monte Carlo implementations: application in mixtures. *Mol. Phys.*, **94**, 519 (1998).

[92] J.N.C. Lopes, D.J. Tildesley. Multiphase equilibria using the Gibbs ensemble Monte Carlo method. *Mol. Phys.*, **92**, 187 (1997).

[93] W.R. Smith, B. Triska. The reaction ensemble method for the computer-simulation of chemical and phase-equilibria. 1. Theory and basic examples. *J. Chem. Phys.*, **100**, 3019 (1994).

[94] M.B. Sweatman, N. Quirke. Simulating fluid—solid equilibrium with the Gibbs ensemble. *Mol. Sim.*, **30**, 23 (2004).

[95] A.Z. Panagiotopoulos, N. Quirke, M. Stapleton, D.J. Tildesley. Phase-equilibria by simulation in the Gibbs ensemble—alternative derivation, generalization and application to mixture and membrane equilibria. *Mol. Phys.*, **63**, 527 (1988).

[96] S.C. McGrother, K.E. Gubbins. Constant pressure Gibbs ensemble Monte Carlo simulations of adsorption into narrow pores. *Mol. Phys.*, **99**, 955 (1999).

[97] A.Z. Panagiotopoulos. Adsorption and capillary condensation of fluids in cylindrical pores by Monte-Carlo simulation in the Gibbs ensemble. *Mol. Phys.*, **62**, 701 (1987).

[98] M.L. Lastoskie, K.E. Gubbins, N. Quirke. Pore-size heterogeneity and the carbon slit pore—a density functional theory model. *Langmuir*, **9**, 2693 (1993).

[99] W.R. Smith, H.L. Vortler. Monte Carlo simulation of fluid phase equilibria in pore systems: Square-well fluid distributed over a bulk and a slit-pore. *Chem. Phys. Lett.*, **249**, 470 (1996).

[100] A.V. Neimark, P.I. Ravikovitch. Guage cell method for simulation studies of phase transitions in confined systems. *Phys. Rev. E*, **62**, 4611 (2000).

[101] A. Vishnyakov, A.V. Neimark. Studies of liquid-vapour equilibria, criticality, and spinodal transitions in nanopores by the guage cell Monte-Carlo method. *J. Phys. Chem. B*, **105**, 7009 (2001).

[102] K. Kiyohara, T. Spyriouni, K.E. Gubbins, A.Z. Panagiotopoulos. Thermodynamic scaling Gibbs ensemble Monte Carlo: A new method for determination of phase coexistence properties of fluids. *Mol. Phys.*, **89**, 965 (1996).

[103] M. Mehta, D.A. Kofke. Coexistence diagrams of mixtures by molecular simulation. *Chem. Eng. Sci.*, **49**, 2633 (1994).

[104] W.A. Steele. The physical interaction of gases with crystalline solids. *Surf. Sci.*, **36**, 317 (1973).

[105] P.J.F. Harris, A. Burian, S. Duber. High-resolution electron microscopy of a microporous carbon. *Philos. Mag. Lett.*, **80**, 381 (2000).

[106] P.J.F. Harris. Structure of non-graphitising carbons. *Int. Mater. Rev.*, **42**, 206 (1997).

[107] S. Figueroa-Gerstenmaier, F.J. Blas, J.B. Avalos, L.F. Vega. Application of the fundamental measure density functional theory to the adsorption in cylindrical pores. *J. Chem. Phys.*, **118**, 830 (2003).

[108] J.P. Olivier, M.L. Occelli. Surface area and microporosity of pillared interlayered clay (PILC) from a hybrid density functional theory (DFT) method. *J. Phys. Chem. B*, **105**, 623 (2001).

[109] V. Gusev, J.A. O'Brien, N.A. Seaton. A self-consistent method for characterization of activated carbons using supercritical adsorption and grand canonical Monte Carlo simulations. *Langmuir*, **13**, 2815 (1997).

[110] S. Samios, A.K. Stubos, N.K. Kanellopoulos, R.F. Cracknell, G.K. Papadopoulos, D. Nicholson. Determination of micropore size determination from grand canonical Monte Carlo simulations and experimental CO_2 isotherm data. *Langmuir*, **13**, 2795 (1997).

[111] S. Samios, G.K. Papadopoulos, T. Steriotis, A.K. Stubos. Simulation study of sorption of CO_2 and N_2 with application to the characterization of carbon adsorbents. *Mol. Sim.*, **27**, 441 (2001).

[112] M.B. Sweatman, N. Quirke. Gas adsorption in active carbons and the slit-pore model 1: Pure gas adsorption and the isosteric heat. *J. Phys. Chem. B.*, (2004), **109**, 10381 (2005).

[113] A. Papadopoulou, F. van Swol, U.M.B. Marconi. Pore end effects on adsorption hysterisis in cylindrical and slitlike pores. *J. Chem. Phys.*, **97**, 6942 (1992).

[114] E. Kozak, G. Chmiel, A. Patrykiejew, S. Sokolowski. Pore closure effect on adsorption hysterisis in slit-like pores. *Phys. Lett. A*, **189**, 94 (1994).

[115] L.D. Gelb. The ins and outs of capillary condensation in cylindrical pores. *Mol. Phys.*, **100**, 2049 (2002).

[116] J.K. Brennan, T.J. Bandosz, K.T. Thomson, K.E. Gubbins. Water in porous carbons. *Colloid Surface A*, **187**, 539 (2001).

[117] E.A. Muller, F.R. Hung, K.E. Gubbins. Adsorption of water–methane mixtures on activated carbons. *Langmuir*, **16**, 5418 (2000).
[118] S. Qiao, K. Wang, X. Hu. Study of binary adsorption equilibrium of hydrocarbons in activated carbon using micropore size distribution. *Langmuir*, **16**, 5130 (2002).
[119] F. Dreisback, R. Staudt, J.U. Keller. High pressure adsorption data of methane, nitrogen and carbon dioxide and their binary and ternary mixtures on activated carbon. *Adsorption-J. Int. Ads. Soc.*, **5**, 215 (1999).
[120] N.V. Choudhury, R.V. Jasra, S.G.T. Bhat. An improved Langmuir approach for prediction of binary gas–mixture adsorption equilibria. *Sep. Sci. Tech.*, **30**, 2337 (1995).
[121] R. Bai. Effect of energy correlation on multicomponent adsorption equilibria prediction using heterogeneous extended Langmuir model. *Chem. Eng. Sci.*, **55**, 5165 (2000).
[122] G.O. Wood. Review and comparisons of D/R models of equilibrium adsorption of binary mixtures of organic vapours on activated carbons. *Carbon*, **40**, 231 (2002).
[123] K. Nieszporek. On the correct use of the Dubinin-Astakhov equation to study the mixed gas adsorption equilibria. *Adsorption-J. Int. Ads. Soc.*, **8**, 45 (2002).
[124] W.S. Appel, M.D. LeVan, J.E. Finn. Non-ideal adsorption equilibria described by pure component isotherms and virial mixture coefficients. *Ind. Eng. Chem. Res.*, **37**, 4774 (1998).
[125] M. Carsky, D.D. Do. Neural network modelling of adsorption of binary vapour mixtures. *Adsorption*, **5**, 183 (1999).
[126] S.M. Taqvi, M.D. LeVan. Virial description of two-component adsorption on homogeneous and heterogeneous surfaces. *Ind. Eng. Chem. Res.*, **36**, 2197 (1997).
[127] J. Ghassemzadeh, L.F. Xu, T.T. Tsotsis. Statistical mechanics and molecular simulation of adsorption in microporous materials: Pillared clays and carbon molecular sieve membranes. *J. Phys. Chem. B*, **104**, 3892 (2000).
[128] L.F. Xu, T.T. Tsotsis, M. Sahimi. Statistical mechanics and molecular simulation of adsorption of ternary gas mixtures in nanoporous materials. *J. Chem. Phys.*, **114**, 7196 (2001).
[129] A.L. Myers, J.M. Prausnitz. Thermodynamics of mixed-gas adsorption. *AIChE*, **11**, 121 (1965).
[130] J.S. Rowlinson, F.L. Swinton. *Liquids and Liquid Mixtures*, Butterworths, London (1982).
[131] V. Gusev, J.A. Obrien, C.R.C. Jensen, N.A. Seaton. Theory for multicomponent equilibrium: Multispace adsorption model. *AIChE*, **42**, 2773 (1996).
[132] A. Malek, S. Farooq. Comparison of isotherm models for hydrocarbon adsorption on activated carbon. *AIChE*, **42**, 3191 (1996).
[133] N. Sundaram. Equation for adsorption from gas-mixtures. *Langmuir*, **11**, 3223 (1995).
[134] R.F. Cracknell, D. Nicholson. Adsorption of gas mixtures on solid surfaces, theory and computer simulation. *Adsorption*, **1**, 16 (1995).
[135] T. Vuong, P.A. Monson. Monte Carlo simulations of adsorbed solutions in heterogeneous porous materials. *Adsorption*, **5**, 183 (1999).
[136] M.B. Sweatman, N. Quirke. Predicting the adsorption of gas mixtures: density functional theory versus adsorbed solution theory. *Langmuir*, **18**, 10443 (2002).
[137] L.P. Ding, S.K. Bhatia. Application of heterogeneous vacancy solution theory to characterization of microporous solids. *Carbon*, **39**, 2215 (2001).
[138] K. Wang, S.Z. Qiao, X. Hu. Application of IAST in the prediction of multicomponent adsorption equilibrium of gases in heterogeneous solids: Micropore size distribution versus energy distribution. *Ind. Eng. Chem. Res.*, **39**, 527 (2000).
[139] S. Qiao, K. Wang, X. Hu. Using local IAST with micropore size distribution to predict multicomponent adsorption equilibrium of gases in activated carbon. *Langmuir*, **16**, 1292 (2000).
[140] D.P. Valenzuela, A.L. Myers, O. Talu, I. Zwiebel. Adsorption of gas mixtures: Effect of energetic heterogeneity. *AIChE*, **34**, 397 (1988).
[141] K. Wang, S.Z. Qiao, X.J. Hu. On the performance of HIAST and IAST in the prediction of multicomponent adsorption equilibria. *Sep. Purif. Technol.*, **20**, 243 (2000).
[142] R. Van der Vaart, C. Huiskes, H. Bosch, T. Reith. Single and mixed gas adsorption equilibria of carbon dioxide/methane on activated carbon. *Adsorption*, **6**, 311 (2000).
[143] V. Gusev, J.A. O'Brien. Prediction of gas mixture adsorption on activated carbon using molecular simulations. *Langmuir*, **14**, 6328 (1998).
[144] G.M. Davies, N.A. Seaton. Predicting adsorption equilibrium using molecular simulation. *AICHE*, **46**, 1753 (2000).
[145] M. Heuchel, G.M. Davies, E. Buss, N.A. Seaton. Adsorption of carbon dioxide and methane and their mixtures on an activated carbon: Simulation and experiment. *Langmuir*, **15**, 8695 (1999).
[146] M.B. Sweatman, N. Quirke. Gas adsorption in active carbons and the slit-pore model 2: mixture adsorption prediction with DFT and AST. *J. Phys. Chem. B.*, (2004) **109**, 10389 (2005).